Predictability of Apparent Viscosity in a Vibratory Shearing Flow Field

Jin-Ping Qu, Bao-Hua Wei, Zhi-Tao Yang, Yong-Hong Cai

The National Engineering Research Center of Novel Equipment for Polymer Processing, The Key Laboratory of Polymer Processing Engineering of the Ministry of Education, South China University of Technology, Guangzhou 510640, China

Received 9 September 2008; accepted 11 January 2009
DOI 10.1002/app.30145
Published online 14 April 2009 in Wiley InterScience (www.interscience.wiley.com).

ABSTRACT: A self-developed experimental facility by the National Engineering Research Center of Novel Equipment for Polymer Processing, called a *coaxial barrel dynamic rheometer*, was used to test the predictability of the apparent viscosity equations of polymer melts in flat vibrating shear flows. The testing principle of the rheometer is to transform the shear power of a motor and extrusion pressure in a shear field to melt viscosity. The shear field can simulate an orthogonal superposed vibratory flow, boundary vibrating pressure flow, and their combined flow. By comparing equation predictions with experimental results, we show a qualitatively satisfactory and quantitatively reasonable predictive ability, which verifies the work of our mathematical derivations.
© 2009 Wiley Periodicals, Inc. J Appl Polym Sci 113: 1560–1565, 2009

Key words: shear; extrusion; viscosity

INTRODUCTION

Although both the technology of melt vibration in polymer processing and the kinetic theories of non-Newtonian fluids flowing in transient flow fields have been investigated recently by internal external and researchers, kinetic studies of melt vibratory conveying in single-screw dynamic extrusion processing flow fields are still inadequate. One of the most important tasks is to build a constitutive equation describing motions of macromolecules induced by vibration and to resolve high nonlinear and nonlocality kinetic equations of a processing flow field dominated by vibration.

The vibration field is introduced into the whole plasticating and extrusion process so that the plasticating and extrusion for the polymer melt is deeply affected by the vibration force field. As shown by many experimental phenomena, the vibration field decreases the apparent viscosity and elasticity of the polymer melt.[1–9] The combined force field during melt vibratory conveying can be implemented by the flat superposing vibration on steady flow; the flow state of the melt is changed and the bear state of the melt is determined by compounding stress and by control of the amplitude and frequency under a vibration force field in the plasticating and extrusion process.

Osaki[10] investigated the parallel superposed libration in a stabilization shear flow field with a rheometer to determine that the dynamic viscosity and storage modulus decreased with increasing shear velocity.

Tanner and Simmons[11] researched the orthogonal superposed libration in a stabilization shear flow to point out that the dynamic viscosity and storage modulus decreased with increasing shear velocity; it was the same as the parallel superposed libration. The dynamic viscosity and storage modulus decreased with the parallel superposed libration.

Isayev and coworkers[12–15] investigated the parallel superposed libration of small or great amplitude in a stabilization shear flow to determine that the storage modulus and wasting modulus became evidently smaller in low frequency with increasing shear velocity.

Kazakia and Rivlin[16] researched the transformation of the volume flow rate with the parallel or orthogonal superposed libration to detect that the melt conveyed was propitious to the parallel libration. The shear field could simulate orthogonal superposed vibratory flow, boundary vibrating pressure flow, and their combined flow.

In this study, a coaxial barrel dynamic rheometer was used to test the predictability of the apparent

Correspondence to: J.-P. Qu (jpqu@scut.edu.cn).
Contract grant sponsor: National Nature Science Foundation of China; contract grant numbers: 10472034, 10590351.

© 2009 Wiley Periodicals, Inc.

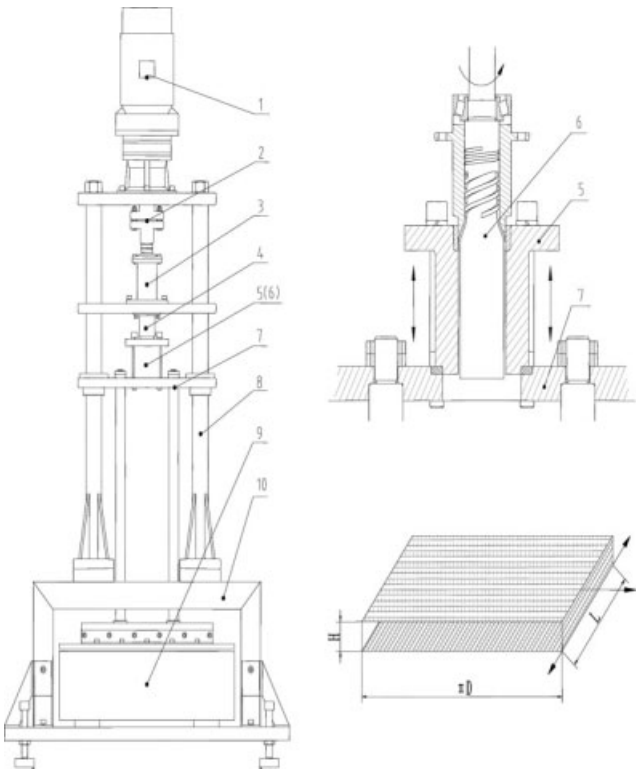

Figure 1 Schematic drawing of the coaxial barrel dynamic rheometer: (1) motor, (2) shaft coupling, (3) bearing block, (4) feed barrel, (5) vibration barrel, (6) special screw, (7) vibration plate, (8) upright column, (9) vibration exciter, and (10) bed.

viscosity equations of polymer melts in flat vibrating shear flows. The testing principle of the rheometer was to transform the shear power of a motor and extrusion pressure in a shear field to melt viscosity. By comparing equation predictions with experimental results, we show a qualitatively satisfactory and quantitatively reasonable predictive ability, which verifies our mathematical derivations.

EXPERIMENTAL

Material and preparation

1. Low-density polyethylene (LDPE) with the trademark 951-050, provided by Mao Ming Petrifaction Ethylene, Ltd. (Mao Ming, China), was used in these experiments. For LDPE, the density and the melt flow index measured under standard test conditions were 0.92 g/cm^3 and 2.196 g/10 min (190°C, 2.16 kgf), respectively.
2. Linear LDPE with the trademark 7144, provided by Da Qing Petrifaction, Ltd. (Da Qing, China), was used in these experiments. For linear LDPE, the density and the melt flow index measured under standard test conditions were 0.92 g/cm^3 and 16.3 g/10 min (190°C, 2.16 kgf), respectively.

Apparatus and methods

A self-developed experimental facility by the National Engineering Research Center of Novel Equipment for Polymer Processing, called a *coaxial barrel dynamic rheometer*, is used to simulate and test the recurrence the polymer melts under a vibrating shear force field in dynamic molding processing. It is made up of a transmission segment, a melt feed conveyed segment, a compound shear segment, and a vibration exciter segment, and its schematic diagram is shown in Figure 1.

Figure 2 shows the principle of the coaxial barrel dynamic rheometer; the polymer melt feed was conveyed to the coaxial barrel dynamic rheometer by a single-screw dynamic extruder. The polymer melt was full of a loop workaround in a compound shear force field when the facility was started up. The testing principle of the rheometer was to transform the shear power of a motor and extrusion pressure in a shear field to melt viscosity. The shear field could simulate an orthogonal superposed vibratory flow, a boundary vibrating pressure flow, and their combined flow. By comparing equation predictions with experimental results, we show a qualitatively satisfactory and quantitatively reasonable predictive ability.

RESULTS AND DISCUSSION

By the technique of the dynamic plasticating extruder, vibration in the axial direction was put on the rotating screw. The shear field could simulate an orthogonal superposed vibratory flow, a boundary vibrating pressure flow, and their combined flow. The melt in the metering section was transported under a vibration force field, and complex shear and

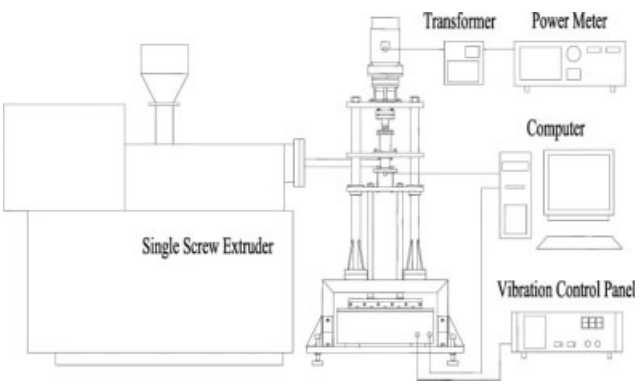

Figure 2 Schematic diagram of the coaxial barrel dynamic rheometer.

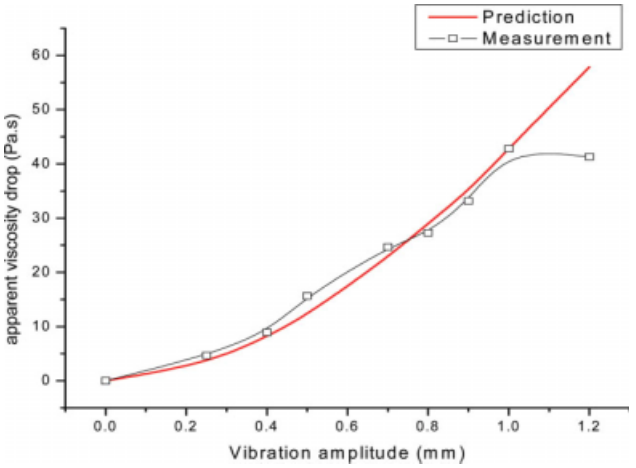

Figure 3 Comparison of the prediction with measurement of the apparent viscosity drop with vibration amplitude at a fixed frequency of 15 Hz. [Color figure can be viewed in the online issue, which is available at www.interscience.wiley.com.]

periodicity pulsant pressure acted on it so as to intensifying mixability and dispersion.

Apparent viscosity of the melt in an orthogonal superposed drag flow field

When the barrel was brought to bear vibration and the mandril started circumrotating, the polymer melt was full of a loop workaround, but so it would not extruded, the melts of the loop workaround came under an orthogonal superposed drag vibration shear. The apparent viscosity of the melt (η'_a) could be forecast as follows in an orthogonal superposed drag flow field:[17]

$$\eta'_a = K\dot{\gamma}_0^{n-1}\left(1+\frac{\varepsilon^2}{2}\right)^{(n-1)/2} \quad (1)$$

where $\dot{\gamma}_0 = \pi DN/H$, $\varepsilon = 2Af/DN$ [n is flow exponent, ε is vibration influence gene, $\dot{\gamma}_0$ is zero shear velocity, A is the amplitude (m), f is the frequency (Hz), D is the diameter of the cylinder (m), N is the rotational speed of the cylinder (rotations/s), and H is the film thickness (m)] and K is a constant. When $\varepsilon = 0$, the vibration parameter is 0, the flow field in a workaround is a simple steady drag flow field, and the apparent viscosity of the melt is η_a^0 ($=K\dot{\gamma}_0^{n-1}$). When $\varepsilon \neq 0$, the increment of the apparent viscosity of the melt is shown as follows with a dynamic flow field relative to a steady flow field:[4–6]

$$\eta_a^0 - \eta'_a = K\dot{\gamma}_0^{n-1}\left[1-\left(1+\frac{\varepsilon^2}{2}\right)^{(n-1)/2}\right] \quad (2)$$

For viscometric performance by power, the increment of the apparent viscosity of the melt may be forecast by the power (P; W), where L is the length of the cylinder (m) P^0_{out} is electrical output power, P'_{out} is electrical output under vibration, and N is not zero:[17]

$$\eta_a^0 - \eta'_a = \frac{H(P^0_{\text{out}} - P'_{\text{out}})}{L\cdot N^2(\pi D)^3(1+\varepsilon^2/4)} \quad (3)$$

Figures 3 and 4 show, respectively, the comparison of the prediction with measurement of the apparent viscosity drop with vibration amplitude at fixed frequencies of 15 and 10 Hz. The apparent viscosity drop increased with increasing vibration amplitude when $A \leq 1.0$ mm and stress amplitude (γ) $= A/H < 0.67$, and the variety trend and numerical value were close to prediction compared with the measurement; this showed that the forecast of the equation was preferable in determining the nature and fixing the quantity. When $A > 1.0$ mm and $\gamma > 0.67$, the measured apparent viscosity dropped placidly; the apparent viscosity had a threshold characteristic over the dynamic displacement amplitudes, and the varying trend could not be predicted by theoretical curve. The apparent viscosity dropped increasingly with increasing vibration frequency, as shown in Figures 3 and 4.

Apparent viscosity of the melt in a boundary vibrating pressure flow field

When barrel was brought to bear vibration and the mandril was still, the polymer melt was extruded steadily from the loop workaround, and the melts of the loop workaround came under boundary vibrating pressure vibration shear. The apparent viscosity of the melt could be forecast as follows in a boundary vibrating pressure flow field:[17]

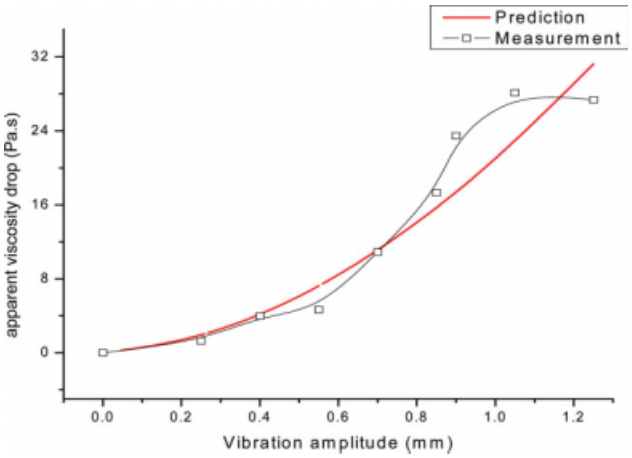

Figure 4 Comparison of the prediction with measurement of the apparent viscosity drop with vibration amplitude at a fixed frequency of 10 Hz. [Color figure can be viewed in the online issue, which is available at www.interscience.wiley.com.]

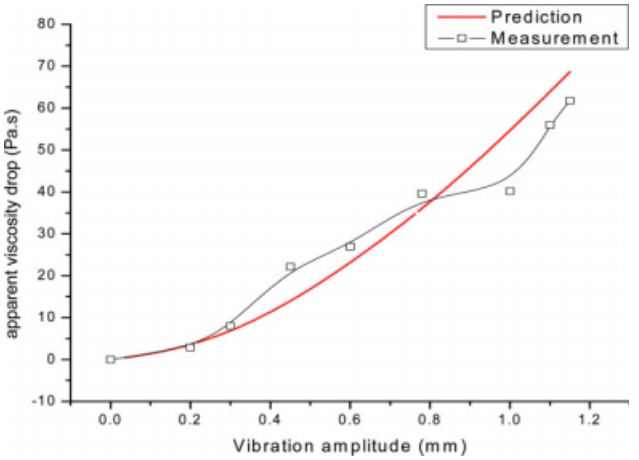

Figure 5 Comparison of the prediction with measurement of the apparent viscosity drop with vibration amplitude at a fixed frequency of 15 Hz. [Color figure can be viewed in the online issue, which is available at www.interscience.wiley.com.]

$$\eta_a' = K\left[\frac{2\bar{Q}}{\pi DH^2}\left(2+\frac{1}{n}\right)\right]^{n-1}\left(1+\frac{\zeta^2}{2}\right)^{(n-1)/2} \times \left(\frac{1+\zeta^2\cos^2\varphi/2}{1+\zeta^2/2}\right)^{1/2} \quad (4)$$

where $\zeta = AHD\pi^2 f/\overline{Q}(2 + 1/n)$, ζ is vibration influence gene, $\overline{Q}$ is the volume flow rate (m^3/s), and ϕ is the phasic difference between the stress and strain. When $\zeta = 0$ and the vibration parameter is 0, the flow field in the workaround is a simple steady pressure flow field, and the apparent viscosity of the melt is η_a^0 $\{= K[2\overline{Q}(2 + 1/n)/\pi DH^2]^{n-1}\}$. When $\zeta \neq 0$, the increment of the apparent viscosity of the melt is shown as follows with the dynamic flow field relative to the steady flow field:

$$\eta_a^0 - \eta_a' = K\left[\frac{2\bar{Q}}{\pi DH^2}\left(2+\frac{1}{n}\right)\right]^{n-1}\left[1-\left(1+\frac{\zeta^2}{2}\right)^{(n-1)/2} \times \left(\frac{1+\zeta^2\cos^2\varphi/2}{1+\zeta^2/2}\right)^{1/2}\right] \quad (5)$$

For viscometric performance by pressure, the increment of the apparent viscosity of the melt could be forecast by the pressure (P; Pa) of the melts:[17]

$$\eta_a^0 - \eta_a' \approx \frac{(P^0 - \bar{P}')\pi DH^3}{2\bar{Q}L'(2+1/n)} \quad (6)$$

Figures 5 and 6 show, respectively, the comparison of the prediction with measurement of the apparent viscosity drop with vibration amplitude at fixed frequencies of 15 and 10 Hz. The apparent viscosity drop increasingly with increasing vibration amplitude in a dynamic flow field; the varying trend could be closely predicted by the theoretical curve to show that the forecast of the equation was preferable in determining the nature and fixing quantity. When $A > 1.0$ mm and $\gamma > 0.67$, Figure 6 shows that the measurement apparent viscosity dropped placidly. The varying trend could be not predicted by the theoretical curve. Figures 5 and 6 show the trend of the apparent viscosity drop with vibration amplitude change at various frequencies. The change in the apparent viscosity drop was closely predicted by the theoretical curve under a boundary vibrating pressure flow field.

Apparent viscosity of the melt in an orthogonal superposed combined flow field

When the barrel was brought to bear vibration and the mandril was circumrotated by the motor, the polymer melt was extruded steadily from the loop workaround, and the melts of the loop workaround came under orthogonal superposed drag vibration shear and pressure vibration shear. The apparent viscosity of the melt could be forecast as follows in an orthogonal superposed combined flow field:[17]

$$\eta_a' = K\left\{\left[\left(\frac{\pi DN}{H}\right)^2 + \left(\frac{2\bar{Q}}{\pi DH^2}\right)^2\left(2+\frac{1}{n}\right)^2\right]\left(1+\frac{\zeta^2}{2}\right)\right\}^{(n-1)/2} \times \left(\frac{1+\zeta^2\cos^2\varphi/2}{1+\zeta^2/2}\right)^{1/2} \quad (7)$$

where $\zeta = AHD\pi^2 f/\overline{Q}(2 + 1/n)$. When $\zeta = 0$ and vibration parameter is 0, the flow field in the workaround is a steady combined flow field of drag flow and pressure flow, and the apparent viscosity of the melt is

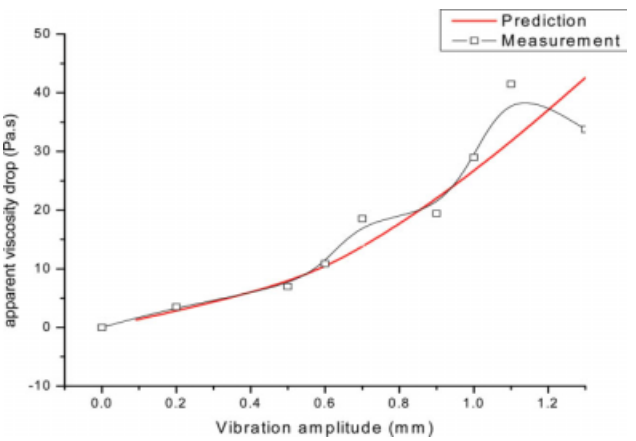

Figure 6 Comparison of the prediction with measurement of the apparent viscosity drop with vibration amplitude at a fixed frequency of 10 Hz. [Color figure can be viewed in the online issue, which is available at www.interscience.wiley.com.]

$$\eta_a^0 = K\left(\dot{\gamma}_d^2 + \dot{\gamma}_p^2\right)^{(n-1)/2} \tag{8}$$

where[4–9]

$$\dot{\gamma}_d = \frac{\pi DN}{H}$$
$$\dot{\gamma}_p = \frac{2\bar{Q}}{\pi DH^2}\left(2 + \frac{1}{n}\right) \tag{9}$$

Thus, when $\zeta \neq 0$, the increment of the apparent viscosity of the melt is shown as follows with the dynamic flow field relative to the steady flow field:[4–10]

$$\eta_a^0 - \eta_a' = K\left(\dot{\gamma}_d^2 + \dot{\gamma}_p^2\right)^{(n-1)/2} \times \left[1 - \left(1 + \frac{\zeta^2}{2}\right)^{(n-1)/2}\left(\frac{1 + \zeta^2\cos^2\varphi/2}{1 + \zeta^2/2}\right)^{1/2}\right] \tag{10}$$

For viscometric performance by power, the increment of the apparent viscosity of the melt may be forecast by the power, where N is not zero:[4–11,17]

$$\eta_a^0 - \eta_a' = \frac{H(P_{out}^0 - P_{out}')}{(\pi D)^2 L \cdot N\sqrt{\dot{\gamma}_d^2 + \dot{\gamma}_p^2}} \tag{11}$$

Figures 7 and 8 show, respectively, the comparison of the prediction with measurement of the apparent viscosity drop with vibration amplitude at fixed frequencies of 15 and 10 Hz. The apparent viscosity dropped increasingly with increasing vibration amplitude when $A \leq 1.00$ mm and $\gamma = A/H < 0.67$, and the variety trend and numerical value were close to prediction compared with measurement. This showed that the forecast of the equation was preferable in determining the nature and fixing quantity. When $A > 1.0$ mm and $\gamma > 0.67$, the measured apparent viscosity dropped placidly, and the varying trend could not be predicted by the theoretical curve. The apparent viscosity dropped increasingly with increasing vibration frequency, as shown in Figures 7 and 8.

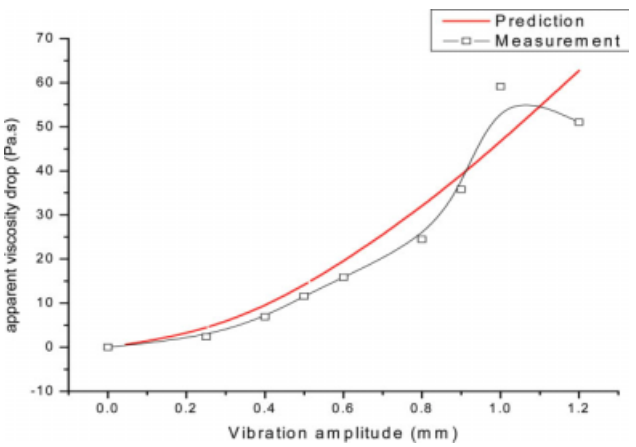

Figure 7 Comparison of the prediction with measurement of the apparent viscosity drop with vibration amplitude at a fixed frequency of 15 Hz. [Color figure can be viewed in the online issue, which is available at www.interscience.wiley.com.]

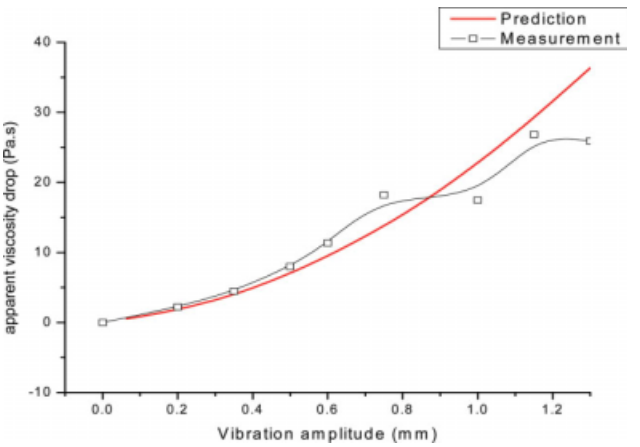

Figure 8 Comparison of the prediction with measurement of the apparent viscosity drop with vibration amplitude at a fixed frequency of 10 Hz. [Color figure can be viewed in the online issue, which is available at www.interscience.wiley.com.]

CONCLUSIONS

By use of measurement in a dynamic viscometric experiment for LDPE, in this study, the viscidity of viscoelastic fluid in several classical cases of flat vibrating shear flows, such as an orthogonal superposition of vibration and steady flow, a boundary vibrating pressure flow, and their combined flows, was studied, and the apparent viscosities of the polymer melts in these flows were deduced, too. By comparing equation predictions with experimental results, we showed a qualitatively satisfactory and quantitatively reasonable predictive ability; as a result of experiment equipment faultiness, the viscometric way by pressure had an error. The production of the error between theory and measurement was analyzed, and prevention measures were discussed.

The authors thank Yonghong Cai for assistance in the experiment.

References

1. Ibar, J. P. Polym Plast Technol Eng 1981, 17, 11.
2. Jingping, Q.; Baiping, X. Plast Rubber Compos 2002, 31, 432.
3. Jingping, Q. Polym Plast Technol Eng 2002, 41, 115.
4. Zhang, J.; Shen, K.; Yuegin, G.; Yuan, Y. J Appl Polym Sci 2005, 96, 818.

5. Zhen, Q., Shangguang, Y.; Lifang, T.; Pen, M. J Appl Polym Sci 2004, 94, 2187.
6. Zheng Yan, K. Z. S.; Zhang, J. J Appl Polym Sci 2003, 91, 1514.
7. Liu, G.; Li, H. J Appl Polym Sci 2003, 89, 2628.
8. Zheng Yan, K. Z. S.; Zhang, J.; Chen, L. M.; Zhou, C. J Appl Polym Sci 2002, 85, 1587.
9. Wang, K.; Zhou, C.; Yu, W. J Appl Polym Sci 2002, 85, 92.
10. Osaki, K. J. Phys Chem 1963, 12, 339.
11. Tanner, R. I.; Simmons, J. M. Chem Eng Sci 1967, 22, 1803.
12. Isayev, A. I.; Wong, C. M. J Polym Sci Part B: Polym Phys 1988, 26, 2303.
13. Isayev, A. I.; Wong, C. M. Adv Polym Technol 1990, 10, 31.
14. Isayev, A. I.; Wong, C. M.; Zeng, X. J Non-Newtonian Fluid Mech 1990, 34, 375.
15. Sobhanie, M.; Isayev, A. I. J Non-Newtonian Fluid Mech 1999, 85, 189.
16. Kazakia, J. Y.; Rivlin, R. S. Rheol Acta 1978, 17, 210.
17. Yonghong, C. Ph.D. dissertation, South China University of Technology, 2006.